

MRS Proc. in press (1990).

CONF-891119--123

Proceedings of the Mater. Res. Soc. -  
Boston, MA, November 1989

DE90 010071

MAY 0 4 1990

STUDIES ON ION SCATTERING AND SPUTTERING PROCESSES RELEVANT TO ION BEAM  
SPUTTER DEPOSITION OF MULTICOMPONENT THIN FILMS

O. AUCIELLO<sup>1,2</sup>, M. S. AMEEN<sup>1</sup>, A. R. KRAUSS<sup>3</sup>, A. I. KINGON<sup>1</sup>, and M. A. RAY<sup>3</sup>  
<sup>1</sup>N. C. State University, Department of Materials Science and Engineering, Raleigh, NC 27695  
<sup>2</sup>Microelectronics Center of North Carolina, Research Triangle Park, NC 27709-2889  
<sup>3</sup>Argonne National Laboratory, Chemistry Division, Argonne, IL 36409

ABSTRACT

Results from computer simulation and experiments on ion scattering and sputtering processes in ion beam sputter deposition of high  $T_c$  superconducting and ferroelectric thin films are presented. It is demonstrated that scattering of neutralized ions from the targets can result in undesirable erosion of, and inert gas incorporation in, the growing films, depending on the ion/target atom mass ratio and ion beam angle of incidence/target/substrate geometry. The studies indicate that sputtering by  $Kr^+$  or  $Xe^+$  ions is preferable to the most commonly used  $Ar^+$  ions, since the undesirable phenomena mentioned above are minimized for the first two ions. These results are used to determine optimum sputter deposition geometry and ion beam parameters for growing multicomponent oxide thin films by ion beam sputter-deposition.

INTRODUCTION

Ion beam sputter deposition has been used to produce multicomponent thin films from sputtering of either multicomponent<sup>1,2</sup> or elemental target materials<sup>3</sup> for a variety of applications. This deposition technique is attractive in that it offers independent control over important parameters such as bombarding species, energy, and system geometry. There exists, however, a need to understand the fundamental ion beam-target/substrate interactions that are occurring during deposition. These processes, which include ion scattering from the target, high energy recoil sputtering, resputtering of the deposited film, and neutralized scattered ion incorporation into the film, are generally undesirable, uncontrolled and may result in degraded film properties.

In this paper, selected results are presented on experimental studies on ion-target/substrate interactions for target materials used to produce  $YBa_2Cu_3O_{7-x}$  superconducting films and electrooptic films. These multicomponent materials possess complex structures and require strict control of processing conditions in order to obtain high quality films with the desired electronic or optical properties. In particular, an understanding of processes affecting stoichiometry, film microstructure, and defect and impurity incorporation is necessary for production of multicomponent films. Our group has recently proven that a computer-controlled ion beam sputter deposition system, which uses a single high current ion beam and elemental target materials on a rotatable target holder, can be used to produce both  $YBa_2Cu_3O_{7-x}$  and  $KNbO_3$  films<sup>3,4</sup> with precise control of the cation stoichiometry. In this technique, metallic or the corresponding oxide targets are sequentially exposed to the ion beam through the computer-controlled rotation of the target holder driven by a stepping motor. The use of elemental metals or judiciously chosen single oxides results in the elimination of undesirable preferential sputtering, characteristic of many complex multielement target materials presently used to produce multicomponent oxide films. However, a need still exists for a thorough understanding of the ion scattering and sputtering phenomena occurring during film deposition. We have examined the sputter yield of various elemental and oxide precursor materials, the deposition rate of these materials at various ion beam parameters, and the amount of gas trapping occurring in the film during deposition. The experimental results have been compared to calculations performed using the TRIM code<sup>5</sup> in order to determine dominant effects and optimize deposition parameters.

DISCLAIMER

This report was prepared as an account of work sponsored by an agency of the United States Government. Neither the United States Government nor any agency thereof, nor any of their employees, makes any warranty, express or implied, or assumes any legal liability or responsibility for the accuracy, completeness, or usefulness of any information, apparatus, product, or process disclosed, or represents that its use would not infringe privately owned rights. Reference herein to any specific commercial product, process, or service by trade name, trademark, manufacturer, or otherwise does not necessarily constitute or imply its endorsement, recommendation, or favoring by the United States Government or any agency thereof. The views and opinions of authors expressed herein do not necessarily state or reflect those of the United States Government or any agency thereof.

MASTER

DISTRIBUTION OF THIS DOCUMENT IS UNLIMITED

## EXPERIMENTAL

Experiments were performed in a turbopumped stainless steel chamber with a base pressure of  $1.0 \times 10^{-7}$  torr. The ion beam was produced by a Kaufman-type ion source with collimated extracting grids. The ion source was typically operated at 1.4 keV and 25 mA, except where noted. High purity Ar, Kr, or Xe gas was introduced via a mass flow controller at 2.0 sccm, resulting in an operating pressure of  $1.0\text{-}5.0 \times 10^{-4}$  torr with the ion beam off. High purity Cu, Y, Ba, and Nb materials were used for the metallic targets, while  $\text{KO}_2$  pellets were made by cold pressing high purity powder in a nitrogen atmosphere.

The measurements were made using the deposition geometry shown in Figure 1. Films were deposited on glass slides or on silicon, in the case of barium, at the  $30^\circ$ ,  $60^\circ$ , and  $90^\circ$  positions indicated in Figure 1, with the target/ion beam angle at either  $45^\circ$  or near normal incidence. Deposition rates were determined either by profilometry of the deposited films or by dynamic measurements with a quartz crystal resonator located in the appropriate position. A comparison of the two techniques yielded identical results for Cu films.

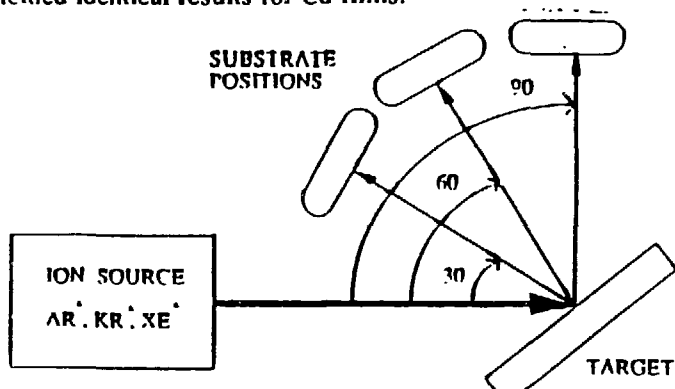


Figure 1. System geometry used for measuring deposition rates and for determining gas trapping. The sketch above shows the ion beam impacting at  $45^\circ$  to the target surface normal.

Gas trapping studies were performed with secondary ion mass spectrometry (SIMS) using a Cameca instrument. Depth profiles of Ar, Kr, and Xe were obtained from different samples, and relative values were established at the  $30^\circ/60^\circ/90^\circ$  positions indicated in Figure 1.

## SPUTTERING AND SCATTERING PROCESSES IN SUPERCONDUCTING FILMS

Figure 2 shows the net deposition rate of Cu and Y for both  $45^\circ$  and near normal ion beam incidence as a function of substrate relative to the incoming ion beam (see Fig. 1). The data indicates a larger net deposition at the  $90^\circ$  position for  $45^\circ$  ion beam incidence. The deposition rate is greater for the case of bombardment with the higher ion mass, as may be expected from sputtering theory<sup>6</sup> and experiments<sup>7</sup>. The reason for the slight increase in the measured deposition rate at the  $90^\circ$  position for the near normal  $\text{Ar}^+$  and  $\text{Kr}^+$  bombardment of Y is presently unclear. Further experiments are being performed to confirm whether this increase is real, as a trend more like the one observed for the Cu case should occur, considering the irradiation geometry and the expected angular distribution of the sputtered flux.

The amount of Ar gas incorporated into the films, as determined by SIMS, is shown in Figure 3. The beam - target angle was  $45^\circ$  with respect to the target normal, as shown in Figure 1. Films were deposited at all positions ( $30^\circ/60^\circ/90^\circ$ ) simultaneously to minimize run-to-run deviations. While this measurement does not give a direct determination of the ion scattering processes that are occurring during deposition, a qualitative understanding may be gained by correlating the data with computer simulations presented below. Inspection of the data in Figure 3 shows that the amount of Ar trapped in the films decreases from the  $90^\circ$  to the  $30^\circ$  position, the effect being stronger for the Ba case. Measurement for  $\text{Xe}^+$  bombardment indicated an almost negligible trapping in the same

materials, while measurements of Kr trapping are underway. The quantification of the SIMS data is, however, difficult, due in part to large matrix effects which may alter the relative intensity of the signal measured.<sup>8</sup> Therefore we here consider only the relative trends observed. A more quantitative study will be undertaken using standard Ar<sup>+</sup> implanted samples.

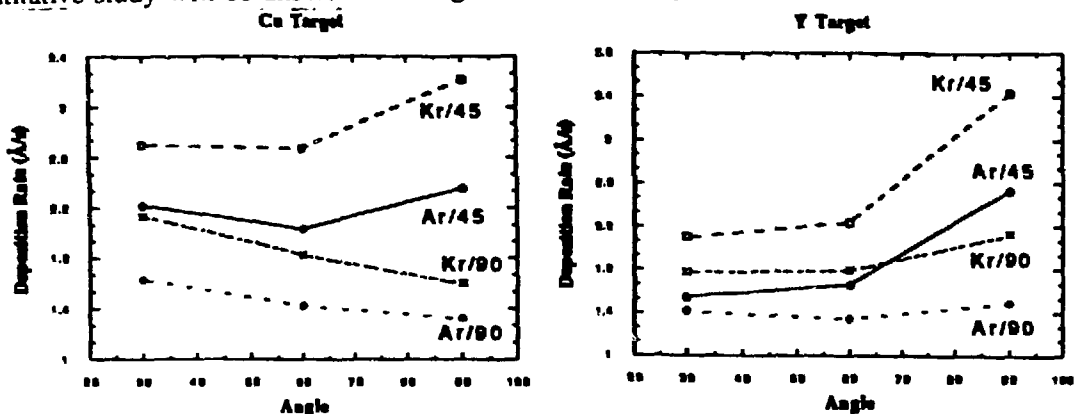


Figure 2. Deposition rate of Cu and Y films at both 45° and normal ion beam incidence at 30°, 60°, and 90° positions relative to the ion beam (See Figure 1).

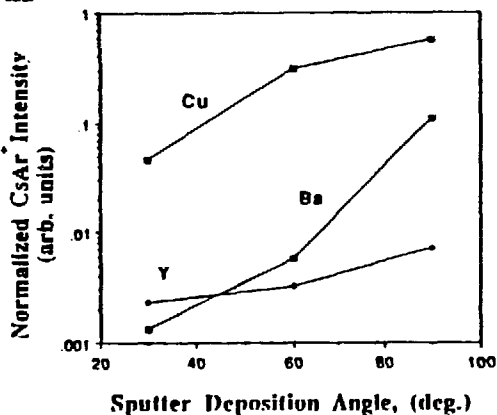


Figure 3. SIMS data showing relative amount of Ar gas incorporated into Cu, Y, and Ba films. Steady-state SIMS count levels were used. The Ar and Ca peaks were not resolvable in the system used for these analyses. Therefore, the CsAr<sup>+</sup> (mass 173) peak was monitored, and energy spectra were taken at various stages during the profiling to assure that a sharp peak, characteristic of the easily dissociable CsAr<sup>+</sup> molecule, was observed, rather than the long tailed peak, which would appear if CsCa molecules were being produced. Details of this analysis will be published elsewhere.

In addition to the experimental results, we have performed computer simulations of the sputtering and scattering processes to establish qualitative correlations with the former. The TRIM code<sup>5</sup> has been used to generate the data presented in Figures 4-5.

Figure 4 shows the results of TRIM calculations for the sputtering yield ( $Y_s$ ) of Y and Cu as a function of the ion beam energy for 45° incidence; the trends for normal incidence being similar, although with slightly lower  $Y_s$  values<sup>9</sup>. The calculations for Ba, not shown here, are very similar to Cu in shape and magnitude<sup>9</sup>. As may be expected,  $Y_s$  depends on the ion/target mass ratio and ion beam angle of incidence. However, the sputter yield for Kr<sup>+</sup> is seen to be closer to that for Xe<sup>+</sup> even though the mass of Kr (80 amu) is nearer to Ar (40 amu) than to Xe (131 amu). This indicates that the sputter yield will probably increase slowly as ion mass increases for these target materials, and only little advantage is gained when increasing the mass of bombarding ions from Kr to Xe.

A calculation for the number of neutralized ions scattered from Ba, as a function of the energy of the scattered species, is shown in Figure 5 for 45° Ar<sup>+</sup> ion beam incidence. This represents the most unfavorable case with respect to ion/target mass ratio. (Calculations for Cu and Y have recently been published elsewhere<sup>9</sup>). The model predicts a significant percentage of high energy (initial beam energy 1.4 keV) Ar species scattered from the Ba, but predicts a smaller number of scattered Kr and Xe species from Ba. This result is to be expected based on the masses of the incident ions and target atoms. The model also predicts a smaller number of high energy Kr and Xe species scattered from both Y and Ba. These scattered energetic species can produce erosion of the

growing films and be incorporated into them, which can affect their stoichiometry, microstructure, and quality.

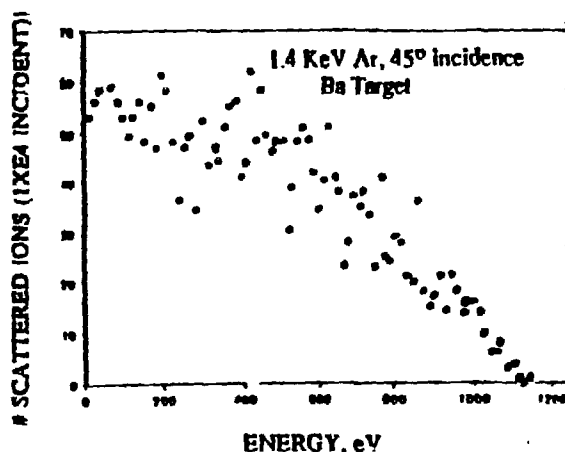
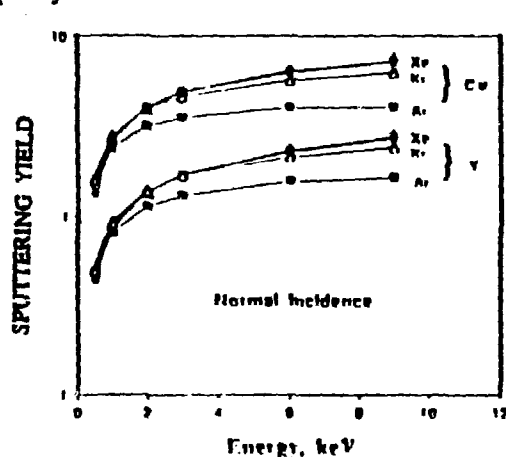


Figure 4. Sputtering Yields ( $Y_s$ ) vs. beam energy for  $\text{Ar}^+$ ,  $\text{Kr}^+$  and  $\text{Xe}^+$  ion bombardment of Cu and Y at  $45^\circ$  beam incidence with respect to the target surface normal.

Figure 5. Ion scattering yield vs. energy of the scattered species for  $\text{Ar}^+$  ion bombardment of Ba at  $45^\circ$  angle of incidence.

#### SPUTTERING AND SCATTERING PROCESSES IN FERROELECTRIC THIN FILMS

The analysis of ion scattering and sputtering of the precursor target materials for the production of ferroelectric  $\text{KNbO}_3$  is presented in a similar fashion to the case of the superconducting material. Further information on the growth and analysis of this material by ion beam sputtering has been published elsewhere<sup>4</sup>. The use of the superoxide  $\text{KO}_2$  as one of the precursors complicates the analysis because of secondary, uncontrolled processes that take place during the sputter erosion of the target. These processes can include target charging, preferential sputtering of a particular element, leading to altered surface stoichiometry, and formation of severe surface morphology. Kelly has reviewed sputtering of oxide materials in detail<sup>8</sup>. We discuss the implications of these processes in the analysis of our experiments and simulations.

The deposition rates of Nb and  $\text{KO}_2$  as a function of substrate position are shown in Figures 6 and 7 respectively. The trend for Nb deposition is similar to that observed in the deposition of metallic materials used for synthesizing high  $T_c$  superconducting films<sup>9</sup>. The deposition rate for the oxide shows much larger scatter in the data than does the metal. The general trend seems to be the same as in the metals, but the error and reproducibility is probably due to factors mentioned in the previous paragraph.

The computer simulations for ion scattering versus the energy of scattered species are presented for Nb and  $\text{KO}_2$  in Figure 8. The deposition rate, and scattering of incident ions from Nb exhibit analogous trends to those observed for the metals related to high  $T_c$  superconducting films. This result is not surprising considering the various masses of the materials involved. The number of scattered Ar species is very small in the case of Ar incident on  $\text{KO}_2$ , indicating very efficient energy transfer to the target atoms for this case. The use of  $\text{Kr}^+$  or  $\text{Xe}^+$  ions minimizes the amount of scattered species, which has led to successful production of relatively high quality epitaxial  $\text{KNbO}_3$  films on (100) MgO. We believe that this success was due to a large extent to an optimized deposition geometry, where undesirable ion scattering effects were minimized.

(and increased gas incorporation). We therefore expect that the sputtering yield will increase faster than the scattering of ions for directions closer to the specular reflection position at  $90^\circ$ .

## CONCLUSIONS

Following the analysis presented above, we can draw conclusions regarding the optimum system geometry and ion beam parameters in order to deposit high quality films by minimizing gas trapping and damage from bombarding species. The sputter rate data indicates that the highest rates are obtained at  $45^\circ$  incidence using  $Xe^+$  ions. However, the difference between the sputtering yields for  $Xe^+$  and  $Kr^+$  ions may not be as substantial as to offset the high cost of the Xe gas. Sputtering with Ar gas results in higher energy neutralized scattered ions from the surface, especially as the mass of the target atom increases. This results in film resputtering and gas incorporation. The scattering process can be reduced by depositing at the  $30^\circ$  position with the beam normal to the target, at a cost of deposition rate. The best compromise may be obtained by using  $Kr^+$  ions at  $45^\circ$  incidence angle to maximize deposition rate, which yields lower energy scattered species and less tendency for trapping than  $Ar^+$  ions. For heavier atomic mass unit target materials, a substrate position nearer  $60^\circ$  may be desirable to minimize any potential ion scattering. Further work will be necessary to quantify the data presented here, and is warranted, considering the impact that these studies may have in optimizing the parameters for the deposition of high quality superconducting films by ion beam sputter-deposition.

## ACKNOWLEDGMENTS

This work was performed with support of the Defense Advanced Research Projects Agency (N-00014-88-K-0525). Partial support was also obtained from the Office of Naval Research (N-00014-88-K-0526), the National Science Foundation (DMR-88-07367), and the Department of Energy (Basic Energy Sciences W-31-109-ENG-38 and DEFG05-88ER-45359). The authors would like to acknowledge the partial technical support of graduate students Tom Graettinger, Clifford Soble, and Y.L. Liu.

## REFERENCES

1. J. M. E. Harper, R. J. Colton, and L. C. Feldman (Eds.), Amer. Inst. Phys. Conf. Proc. 165 (1988).
2. G. Margaritondo, R. Joynt, and M. Onellion (Eds.), Amer. Inst. Phys. Conf. Proc. ~~165~~<sup>182</sup> (1989).
3. A. I. Kingon, O. Auciello, M. S. Ameen, S. H. Rou, and A. R. Krauss, Appl. Phys. Lett. 55, 301 (1989).
4. M. S. Ameen, T. M. Graettinger, O. Auciello, S. H. Rou, A. R. Krauss, and A. I. Kingon, Mat. Res. Soc. Symp. Proc. 152, 175(1989).
5. J. P. Biersack and W. Eckstein, Appl. Phys. A34, 73(1984).
6. P. Sigmund, in "Sputtering by Particle Bombardment I," R. Berisch (Ed.), Springer-Verlag (1981), p. 9.
7. H. H. Andersen and H. L. Bay, in "Sputtering by Particle Bombardment I," R. Berisch (Ed.), Springer-Verlag (1981), p. 145.
8. L. C. Feldman, J. W. Mayer, *Fundamentals of Surface and Thin Film Analysis* (North Holland, New York 1986).
9. M. S. Ameen, O. Auciello, A. I. Kingon, A. R. Krauss, and M. A. Ray, Amer. Inst. Phys. Conf. Proc. (in press, 1990).
10. R. Kelly, Nucl. Inst. and Methods in Phys. Res. B39, 43(1989).